

Thermodynamic Circuits 3: Association of thermoelectric converters in stationary non-equilibrium

Paul Raux,^{1,2} Christophe Goupil,² and Gatién Verley¹

¹*Université Paris-Saclay, CNRS/IN2P3, IJCLab, 91405 Orsay, France*

²*Université Paris Cité, CNRS, LIED, F-75013 Paris, France*

(Dated: December 20, 2024)

We determine the current-force characteristics of the serial (respectively parallel) association of two ThermoElectric Converters (TEC) using the laws of resistance (respectively conductance) matrix addition. Each TEC is modeled by a non-equilibrium conductance/resistance matrix describing the current-force characteristics of the TEC in stationary non-equilibrium. For TECs in series, we investigate the continuity of the potentials (and their derivatives) at their interfaces when thermoelectric coefficients are equal or not. We also study the current-dependent boundary conditions (for each sub-device) that significantly modify the conversion process. For TECs in parallel, we show that our result is compatible with the previously mentioned internal current loops even in open circuit boundary conditions.

I. INTRODUCTION

The connection of thermodynamic conversion devices in networks is a subject that originated in the first half of the last century [1, 2], in the context of the fundamental work of L. Onsager [3]. This disciplinary field experienced a period of strong development in the second half of the century, mainly in biology and bioenergetics [4, 5]. In particular, the work of O. Kedem and R. S. Caplan made it possible to describe coupled transport phenomena across biological membranes under non-equilibrium conditions [6]. Historically, these questions of coupled transport in biology were quickly associated with those of the chemical reactions that govern biochemistry [7]. Beyond the field of biology, thermoelectric conversion [8] is also described using the same force-flow approach. This article focuses on the association of two thermoelectric converter (TEC) that follow the Constant Property Model (CPM) as described in [9]. Although the CPM approach has been highly successful and is still prevalent today, it faces credibility challenges for macroscopic thermoelectric materials where thermodynamic forces exert significant influence. To circumvent this, thermoelectric materials are often discretized into sections, each assumed to follow the CPM. However, for this method to be operational, one must first understand how the matter and energy transport impedances couple at the interface between CPMs of different thermoelectric coefficients. Indeed, in general, macroscopic TECs have space or force-dependent thermoelectric coefficients. This interface problem led in particular to the concept of relative current [10, 11] which highlights the challenge of optimally coupling thermodynamic converters of materials with different transport parameters [10, 12]. This point is central in that it directly questions the adaptation of impedance in the case of nodal structures associating forces and flows of different natures. The multiplicity of coupled flows and forces means that impedance is no longer a scalar but a matrix.

In the present work, we determine effective descriptions for the serial and the parallel association of two TECs by applying respectively the law of resistance matrix addition and the law of conductance matrix addition derived in Ref. [13]. Therefore, given a choice of model for the coupling between the currents, i.e., for a given choice of conductance/resistance matrices, we obtain a unique model for the coupling between the currents of the composite device. We show in particular that under fixed temperature difference, the voltage-current characteristics of the serial association of two TECs (with linear voltage-current characteristics) is non linear. We propose two approaches to explain this non linearity. First, we put forward an effective CPM in which thermoelectric coefficients are function of the electric current. We show that this current-force characteristics for an effective CPM is compatible with the current-force characteristics obtained via the law of resistance matrix addition. Nonetheless the coupling obtained for the effective CPM is different. Second, we show that the TECs within the serial association display a non linear electric response since they are subjected to current dependant boundary conditions (intermediate conditions between Dirichlet and Neumann). This situation is encountered, for example, when modeling the force-velocity response of muscles in animals [14]. We also show that the material property mismatch leads to interface dissipation by Peltier effect: temperature and electric potential are continuous by assumption whereas the composite potentials introduced in Ref. [9] are discontinuous in case of mismatch.

This article is organized as follows. In section II, we briefly recall the CPM conductance matrix for the coupling between the energy and the electric currents in a single TEC. In section III, we derive the nonequilibrium conductance matrix describing the serial association of two TECs by applying the law of resistance matrix addition derived in Ref. [13]. In order to give a physical interpretation of this serial association, we derive an effective

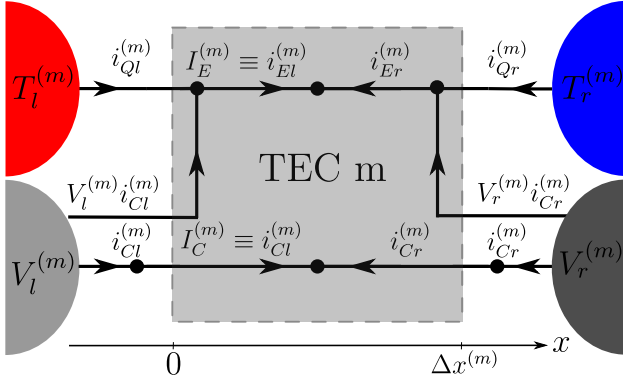


FIG. 1. The TEC is connected to two thermostats at temperature T_l and T_r with $\Delta T = T_r - T_l < 0$ and to two metallic leads at electric potentials V_l and V_r with $\Delta V = V_r - V_l > 0$. At each black dots, the Kirchoff current law applies.

CPM explaining the non linear electric response obtained upon serial association. We also show that every sub-devices within the association is subjected to non ideal boundary conditions. They thus also exhibit non linear voltage current characteristics. We finally interpret as Peltier effect the spatial continuity issues arising at the interface between the two TECs for the various potentials involved (temperature, electric potential, composite potential) for various degrees of mismatch between the thermoelectric coefficients of the subTECs. In section IV, we considers the parallel association of two TEC in Dirichlet boundary conditions (pins of both TECs at the same fixed potentials). We show that in general, the mismatch between the thermoelectric coefficients yields in this case internal currents even in open circuits configurations (no currents from the reservoirs).

II. CONSTANT PROPERTY MODEL

Let us start by recalling the current-force characteristics describing a TEC following the CPM. In Fig. 1, we introduce the notations for the currents exchanged by the TEC with its reservoirs. Current received by the TEC from the reservoir are counted positively. Currents entering the TEC from the $\chi = l, r$ side of device m are: the electric current $i_{C\chi}$, the heat current $i_{Q\chi}$ and the energy current $i_{E\chi}$. The TEC satisfies charge and energy conservation which implies that the electric and energy currents from the left reservoirs are opposed to the ones incoming from the right reservoirs such that we can choose to work with a set of linearly dependant currents $I_E^{(m)}, I_C^{(m)}$:

$$i_{El}^{(m)} = I_E^{(m)} = -i_{Er}^{(m)}, \quad (1)$$

$$i_{Cl}^{(m)} = I_C^{(m)} = -i_{Cr}^{(m)}. \quad (2)$$

$I_E^{(m)}, I_C^{(m)}$ are related to the temperature difference and the voltage applied to the TEC through the following

current-force characteristics

$$I_E^{(m)} = -K^{(m)}\Delta T^{(m)} + F^{(m)}i_{Cl}^{(m)}, \quad (3)$$

$$I_C^{(m)} = -\frac{\alpha^{(m)}\Delta T^{(m)} + \Delta V^{(m)}}{R^{(m)}}, \quad (4)$$

for a given TEC m and where $K^{(m)}$ is the thermal conductivity under zero electric current, $R^{(m)}$ is the isothermal electric resistance, $\alpha^{(m)}$ is the Seebeck coefficient. We also introduced $\Delta T^{(m)} = T_r^{(m)} - T_l^{(m)}, \Delta V^{(m)} = V_r^{(m)} - V_l^{(m)}$ and the free fraction of transported energy

$$F^{(m)} = \alpha^{(m)}\bar{T}^{(m)} + \bar{V}^{(m)}. \quad (5)$$

The average temperature (resp. the average electric potential) of TEC m reads $\bar{T}^{(m)} = (T_l^{(m)} + T_r^{(m)})/2$ (resp. $\bar{V}^{(m)} = (V_l^{(m)} + V_r^{(m)})/2$). This current-force characteristics can be summarized using the conductance matrix derived in Ref. [9] as

$$\begin{pmatrix} i_{El}^{(m)} \\ i_{Cl}^{(m)} \end{pmatrix} = \mathbf{G}^{(m)} \begin{pmatrix} A_E^{(m)} \\ A_C^{(m)} \end{pmatrix}, \quad (6)$$

with

$$\mathbf{G}^{(m)} = \frac{T_l^{(m)}T_r^{(m)}}{R^{(m)}\bar{T}^{(m)}} \begin{bmatrix} K^{(m)}R^{(m)}\bar{T}^{(m)} + F^{(m)2} & F^{(m)} \\ F^{(m)} & 1 \end{bmatrix} \quad (7)$$

and where $A_E^{(m)} = 1/T_r^{(m)} - 1/T_l^{(m)}$ and $A_C^{(m)} = V_l^{(m)}/T_l^{(m)} - V_r^{(m)}/T_r^{(m)}$. The resistance matrix is obtained via the inverse relation $\mathbf{R}^{(m)} = \mathbf{G}^{(m)-1}$ and reads

$$\mathbf{R}^{(m)} = \begin{bmatrix} \frac{1}{K^{(m)}T_l^{(m)}T_r^{(m)}} & -\frac{F^{(m)}}{K^{(m)}T_l^{(m)}T_r^{(m)}} \\ -\frac{F^{(m)}}{K^{(m)}T_l^{(m)}T_r^{(m)}} & \frac{K^{(m)}R^{(m)}\bar{T}^{(m)} + F^{(m)2}}{K^{(m)}T_l^{(m)}T_r^{(m)}} \end{bmatrix}. \quad (8)$$

III. SERIAL ASSOCIATION

In this section, we focus on the serial association of two thermoelectric converters. In Fig. 2, we show how devices 1 and 2 are connected together to give device 3 and how device 3 is connected to its reservoirs (boundary conditions). As mentioned in the introduction, we assume fixed temperature difference $\Delta T^{(3)}$ at the boundaries of device 3. Moreover, energy and electric currents at the interface between TECs 1 and 2 are conserved. This conservation laws can be expressed as

$$I_E^{(1)} = I_E^{(2)} = I_E, \quad (9)$$

$$I_C^{(1)} = I_C^{(2)} = I_C. \quad (10)$$

We also assume that no dissipation occurs at the interface between TECs 1 and 2 which implies the following potential continuity equations:

$$T_r^{(1)} = T_l^{(2)} \equiv T, \quad (11)$$

$$V_r^{(1)} = V_l^{(2)} \equiv V, \quad (12)$$

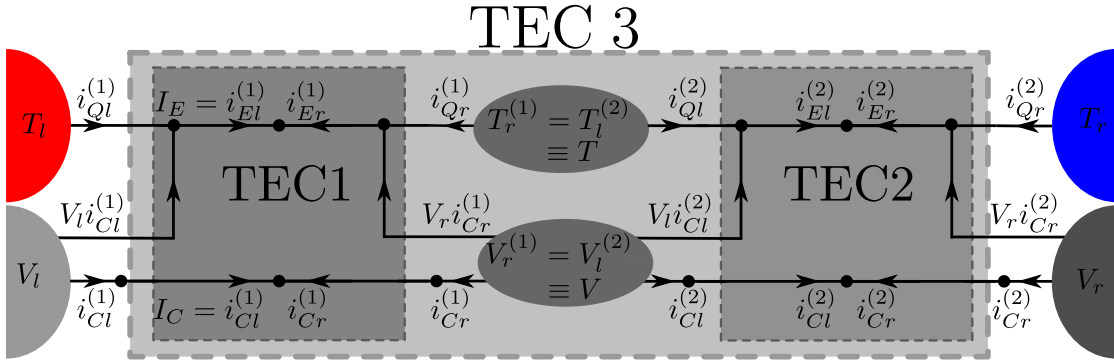


FIG. 2. TEC 3 is connected to two thermostats at temperatures T_l and T_r with $\Delta T^{(3)} = T_r - T_l < 0$ and to two metallic leads at electrical potentials V_l and V_r with $\Delta V^{(3)} = V_l - V_r > 0$. Device 3 is the serial association of TEC 1 and 2. TEC 1 is connected to a heat reservoir at temperature T_l on its left and to the thermal pin of TEC 2 on the right. This imposes a temperature T between the two TEC that depends on the operating point. Similarly, it is connected to a metallic lead on its left which set electrical potential to V_l and to the other TEC on the right which sets a current dependant electrical potential V . The situation for TEC 2 is the left-right symmetric. The sum of currents (incoming arrows) at each black bullet is zero.

where we have introduced T the local temperature and V the electric potential at the interface to shorten notation.

We start this section by the determination of T and V . Then, we determine the equivalent conductance matrix describing the current-force characteristics of TEC 3 by using the law of resistance matrix addition [13]. We show that this conductance matrix is compatible with the one of a CPM like model with current dependant thermoelectric coefficients.

A. Internal local potentials

We start by the determination of T . Combining the energy currents Eq. (3) with the conservation of energy at the interface Eq. (9), we obtain

$$\left(K^{(1)} + K^{(2)}\right) T - \left(K^{(1)} T_l + K^{(2)} T_r\right) = \left(F^{(1)} - F^{(2)}\right) I_C \quad (13)$$

Using the definition of $F^{(m)}$ for $m = 1, 2$ introduced in Eq. (5), we simplify $F^{(1)} - F^{(2)}$ as

$$F^{(1)} - F^{(2)} = \alpha^{(1)} \bar{T}^{(1)} - \alpha^{(2)} \bar{T}^{(2)} - \Delta V^{(3)}. \quad (14)$$

Then using the local potential continuity at the interface and the expression of the electric current Eq. (4), we express $\Delta V^{(3)}$ as

$$\Delta V^{(3)} = - \sum_{m=1}^2 \left(R^{(m)} I_C + \alpha^{(m)} \Delta T^{(m)} \right) \quad (15)$$

Inserting this last equation in Eq. (14) yields

$$F^{(1)} - F^{(2)} = -\delta\alpha T + \frac{R^{(1)} + R^{(2)}}{2} I_C \quad (16)$$

where $\delta\alpha = \alpha^{(2)} - \alpha^{(1)}$. Finally, by inserting this last relation in Eq. (13) and solving for T yields

$$T = \frac{K^{(1)} T_l + K^{(2)} T_r + \frac{R^{(1)} + R^{(2)}}{2} I_C^2}{K^{(1)} + K^{(2)} + \delta\alpha I_C}. \quad (17)$$

Requiring $T > 0$ leads to two inequalities according to the sign of $\delta\alpha$:

$$I_C > - \frac{K^{(1)} + K^{(2)}}{\delta\alpha} \text{ if } \delta\alpha > 0, \quad (18)$$

$$I_C < - \frac{K^{(1)} + K^{(2)}}{\delta\alpha} \text{ if } \delta\alpha < 0. \quad (19)$$

Similarly, interface electric potential V follows from using Eq. (4) in Eq. (10) since $\Delta V^{(1)} = V - V_l$ and $\Delta V^{(2)} = V_r - V$, leading to

$$V = R_{\parallel} \left(\frac{V_l}{R^{(1)}} + \frac{V_r}{R^{(2)}} + \frac{\alpha^{(2)} \Delta T^{(2)}}{R^{(2)}} - \frac{\alpha^{(1)} \Delta T^{(1)}}{R^{(1)}} \right) \quad (20)$$

where $R_{\parallel} = R^{(1)} R^{(2)} / (R^{(1)} + R^{(2)})$. We emphasize that it depends on I_C via T in $\Delta T^{(m)}$ for $m = 1, 2$. We see that the devices 1 and 2 have electrical current dependant local potential differences at their boundaries even though device 3 is in Dirichlet boundary conditions.

B. Law of resistance matrix addition

The law of resistance matrix derived in Ref. [13] yields the resistance matrix $\mathbf{R}^{(3)}$ describing the force-current characteristics

$$\begin{pmatrix} \frac{1}{T_r} - \frac{1}{T_l} \\ \frac{V_l}{T_l} - \frac{V_r}{T_r} \end{pmatrix} = \mathbf{R}^{(3)} \begin{pmatrix} I_E \\ I_C \end{pmatrix} \quad (21)$$

where

$$\mathbf{R}^{(3)} = \mathbf{R}^{(1)} + \mathbf{R}^{(2)}. \quad (22)$$

We provide the detailed derivation of $\mathbf{R}^{(3)}$ in Appendix A 3. Combining Eq. (A31) and Eq. (22), we then obtain the the detailed expression of $\mathbf{R}^{(3)}$ in terms of the properties of 1 and 2

$$\mathbf{R}^{(3)} = \sum_{m=1}^2 \begin{bmatrix} \frac{1}{K^{(m)}T_l^{(m)}T_r^{(m)}} & -\frac{F^{(m)}}{K^{(m)}T_l^{(m)}T_r^{(m)}} \\ -\frac{F^{(m)}}{K^{(m)}T_l^{(m)}T_r^{(m)}} & \frac{K^{(m)}R^{(m)}T_l^{(m)} + F^{(m)2}}{K^{(m)}T_l^{(m)}T_r^{(m)}} \end{bmatrix} \quad (23)$$

$\mathbf{R}^{(3)}$ is positive definite since $\mathbf{R}^{(m)}$ is positive definite for $m = 1, 2$, in accordance with the positivity of the Entropy Production Rate (EPR). Note also that the complexity of the expression of $\mathbf{R}^{(3)}$, because of the dependencies on T and V , makes difficult to draw any physical interpretation. To circumvent this issue, we show that TEC 3 can be modeled by an effective CPM with I_C dependant thermoelectric coefficients. To do so, we introduce the following averages and differences of the thermoelectric coefficients of devices 1 and 2

$$\bar{\alpha} = \frac{\alpha^{(1)} + \alpha^{(2)}}{2}, \quad \delta_{\alpha} = \alpha^{(2)} - \alpha^{(1)}, \quad (24)$$

$$\bar{K} = \frac{K^{(1)} + K^{(2)}}{2}, \quad \delta_K = K^{(2)} - K^{(1)}, \quad (25)$$

$$\bar{R} = \frac{R^{(1)} + R^{(2)}}{2}, \quad \delta_R = R^{(2)} - R^{(1)}, \quad (26)$$

which combined with Eqs. (3-4), yields the following currents through device 3 as

$$I_E = \frac{I_E^{(1)} + I_E^{(2)}}{2} = -K^{(3)}\Delta T^{(3)} + F^{(3)}I_C, \quad (27)$$

$$I_C = \frac{I_C^{(1)} + I_C^{(2)}}{2} = -\frac{\alpha^{(3)}\Delta T^{(3)} + \Delta V^{(3)}}{R^{(3)}}, \quad (28)$$

with the following thermoelectric coefficients for device 3

$$\alpha^{(3)} = \bar{\alpha} - \frac{\delta_{\alpha}}{2(2\bar{K} + \delta_{\alpha}I_C)}, \quad (29)$$

$$K^{(3)} = \frac{\bar{K}}{2} - \frac{\delta_K\delta_{\alpha}}{4(2\bar{K} + \delta_{\alpha}I_C)}, \quad (30)$$

$$R^{(3)} = 2\bar{R} + \delta_{\alpha}\frac{\delta_{\alpha}\bar{T}^{(3)} - \bar{R}I_C}{2\bar{K} + \delta_{\alpha}I_C}, \quad (31)$$

$$F^{(3)} = \frac{F^{(1)} + F^{(2)}}{2} - \frac{\delta_K(\delta_{\alpha}\bar{T}^{(3)} - \bar{R}I_C)}{2(2\bar{K} + \delta_{\alpha}I_C)}. \quad (32)$$

Since we consider an imposed $\Delta T^{(3)}$ value, we see that all these four parameters now depend on the value of the electric current I_C . According to equation Eq. (7), the current-force characteristics of device 3 can thus be described by the conductance matrix $\mathbf{R}^{(3)'}$ which reads

$$\mathbf{R}^{(3)'} = \frac{1}{K^{(3)}T_lT_r} \begin{bmatrix} 1 & -F^{(3)} \\ -F^{(3)} & KR\bar{T}^{(3)} + F^{(3)2} \end{bmatrix} \quad (33)$$

for the force and current basis introduced in Eq. (21). Clearly, this last result does not coincides with the result

obtained by the law of resistance matrix addition. However, since $\mathbf{R}^{(3)'}\mathbf{I} = \mathbf{R}^{(3)}\mathbf{I}$, these matrices satisfy the following relation

$$\mathbf{R}^{(3)'} = \mathbf{R}^{(3)} + \left(R_{22}^{(3)'} - R_{22}^{(3)}\right) \begin{bmatrix} -\left(\frac{I_C}{I_E}\right)^2 & \frac{I_C}{I_E} \\ \frac{I_C}{I_E} & 1 \end{bmatrix} \quad (34)$$

and thus belong to the same class of conductance matrix since they define the same current-force characteristics [15].

In the limit in which TEC 1 and 2 are identical TEC, i.e., with $\alpha^{(1)} = \alpha^{(2)} = \alpha$, $K^{(1)} = K^{(2)} = K$ and $R^{(1)} = R^{(2)} = R$ and of same length, the effective CPM like thermoelectric coefficients reduce to

$$K^{(3)} = K/2, \quad (35)$$

$$R^{(3)} = 2R, \quad (36)$$

$$\alpha^{(3)} = \alpha. \quad (37)$$

This result is expected physically for the serial association of both thermal and electric resistors.

C. Discussion

a. Non linear voltage-current characteristics Fig. 3 shows the temperature differences and voltages applied to the devices 1, 2 and 3. From the derivation of the effective CPM for TEC 3, we can express its voltage-current characteristics as

$$\Delta V^{(3)} = -\left(\alpha^{(3)}\Delta T^{(3)} + R^{(3)}I_C\right) \quad (38)$$

Clearly, since $\alpha^{(3)}$ and $R^{(3)}$ are both functions of the electric current I_C [see Eqs.(29) and (31)], the voltage-current characteristics of TEC 3 is non linear under fixed temperature difference $\Delta T^{(3)}$. Since a single TEC has constant thermoelectric coefficient, it has a linear voltage-current characteristics under fixed temperature difference $\Delta T^{(m)}$ for $m = 1, 2$. Under fixed $\Delta T^{(m)}$, a single TEC is thus analogous to a Thévenin voltage source (ideal voltage source serially connected to a resistor). The serial association of two Thévenin voltage sources would lead to a linear equivalent voltage-current characteristics in the absence of coupling with energy. We thus interpret the emerging non linearity as the result between the coupling between energy and charge currents.

To investigate this coupling, we open device 3 to take a look at the boundary conditions applied to devices 1 and 2 within the serial association. The left panel of Fig. 3 shows the temperature differences on device $m = 1, 2, 3$ as a function of I_C . By assumption, $\Delta T^{(3)}$ is constant. To accomodate this constraint, the temperature differences applied to devices 1 and 2 are non linear functions of I_C . The right panel of Fig. 3 shows that the voltage-current characteristics of devices $m = 1, 2, 3$ are all non linear functions of I_C , as aforementioned for devices 3.

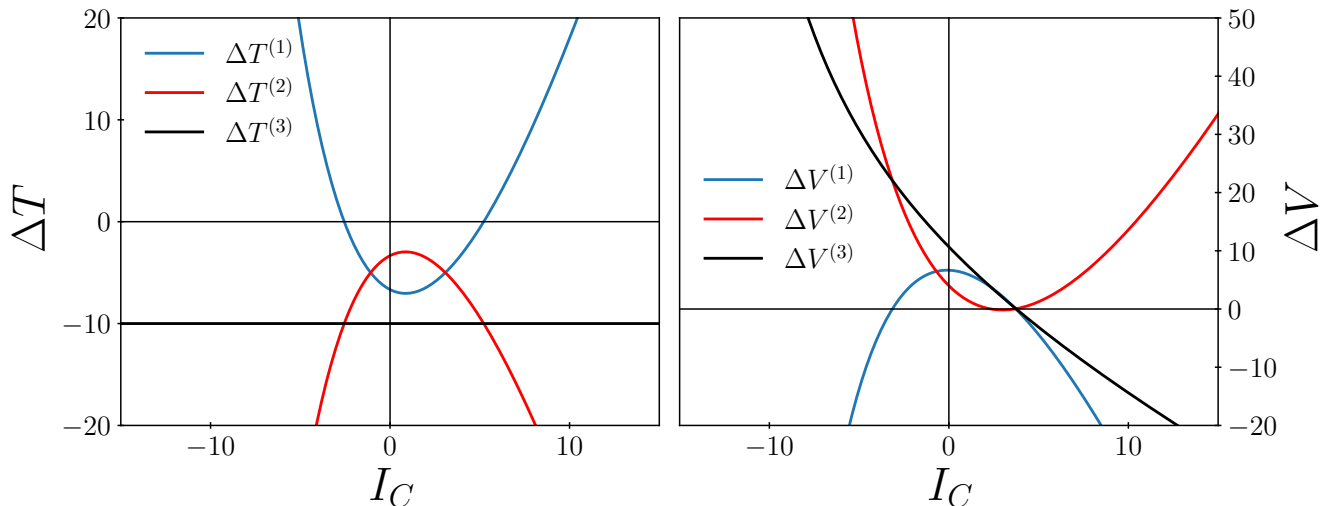


FIG. 3. (Left panel) Temperature T at the interface between TEC 1 and 2 (black dashed line) and temperature differences at the boundary of each TEC: $\Delta T^{(1)}$ (blue solid line), $\Delta T^{(2)}$ (red solid line) and $\Delta T^{(3)}$ (black solid line). (Right panel) Electric potential V at the interface between TEC 1 and 2 (black dashed line) and electric voltage to which each TEC is subjected: $\Delta V^{(1)}$ (blue solid line), $\Delta V^{(2)}$ (red solid line) and $\Delta V^{(3)}$ (black solid line). Temperatures and voltages are shown as function of the electric current I_C at fixed $\Delta T^{(3)} < 0$. For both panels, parameters are: $K^{(1)} = 1, K^{(2)} = 2, R^{(1)} = 1, R^{(2)} = 2, \alpha^{(1)} = 1, \alpha^{(2)} = 1.2, T_l = 20, T_r = 10$ and $V_l = 10$.

For devices 1 and 2, the non-linearity of $\Delta V^{(1)}$ and $\Delta V^{(2)}$ are due to the I_C dependent $\Delta T^{(1)}$ and $\Delta T^{(2)}$. Devices 1 and 2 are thus no longer analogous to Thévenin voltage sources.

Therefore, the interplay between the energy/charge coupling and non ideal boundary conditions, creates complex behaviors for TECs 1, 2 and 3. For now, we didn't take into account the spatial profiles of thermoelectric coefficients. We do so below by considering the spatial evolution of the potentials (temperature, electric potential, composite potentials) across each TEC.

b. Peltier effect at the interface For a given TEC following the CPM [9], the charge and energy currents derive from composite potentials as

$$I_C^{(m)} = -\frac{\Delta x^{(m)}}{R^{(m)}} \frac{d\varphi^{(m)}}{dx}, \quad (39)$$

$$I_E^{(m)} = -K^{(m)} \Delta x^{(m)} \frac{d\Phi^{(m)}}{dx}, \quad (40)$$

where

$$\varphi^{(m)}(x) = \alpha^{(m)} T^{(m)}(x) + V(x), \quad (41)$$

$$\Phi^{(m)}(x) = T^{(m)}(x) + \frac{\varphi^{(m)2}(x)}{2K^{(m)}R^{(m)}}. \quad (42)$$

We show on Fig. 4 the profiles of T , V , φ and Φ . Their analytical expressions are given in Appendix. A 1. In the case of homogeneous system (column A), and due to the conservation of energy and matter, i.e., $I_E(x) = cte$ and $I_C(x) = cte$, the profile of φ and Φ are strictly linear as expected from Eqs. (41–42). Considering in addition

Eqs. (39–40) we see that $\alpha \frac{dT}{dx} + \frac{dV}{dx} = cte$, leading to a similar profiles for $T(x)$ and $V(x)$. We can usefully add the Gibbs-Duhem expression linking energy, heat and carrier currents

$$I_Q(x) = I_E - eV(x)I_C = \left(-K \frac{d\Phi}{dx} + \frac{eV}{R} \frac{d\varphi}{dx} I_C \right) \Delta x, \quad (43)$$

where e is the charge of the carrier. Although not plotted, we can immediately see that the profile of $I_Q(x)$ is simply given by an affine function of $V(x)$. This naturally leads to the result $dI_Q = -e dV(x)I_C$, which translates the conversion of heat into work on a local scale. Note that any non-derivability or discontinuity in $V(x)$ will immediately result in a modification of the system's heat balance and heat-to-work conversion.

The situation of non-derivability of $V(x)$ appears in the case (column B) where the thermal and electrical conductivity terms differ, while maintaining the same Seebeck coefficient in devices (1) and (2). In this case, we observe a slope break without discontinuity between the φ and Φ potentials. The balance given by the Gibbs-Duhem equation is therefore simply modified by the slope breaks.

In the case (column C) where there is a difference between the values of the Seebeck coefficients between devices (1) and (2), the consequence is much greater. Knowing that the Seebeck coefficient is a measure of entropy per carrier $S_N = e\alpha$, it follows that any change in the value of the Seebeck coefficient translates into a modification of the energy balance, which must take this jump in entropy per carrier into account. This situation is well known in thermoelectricity, as it is nothing less

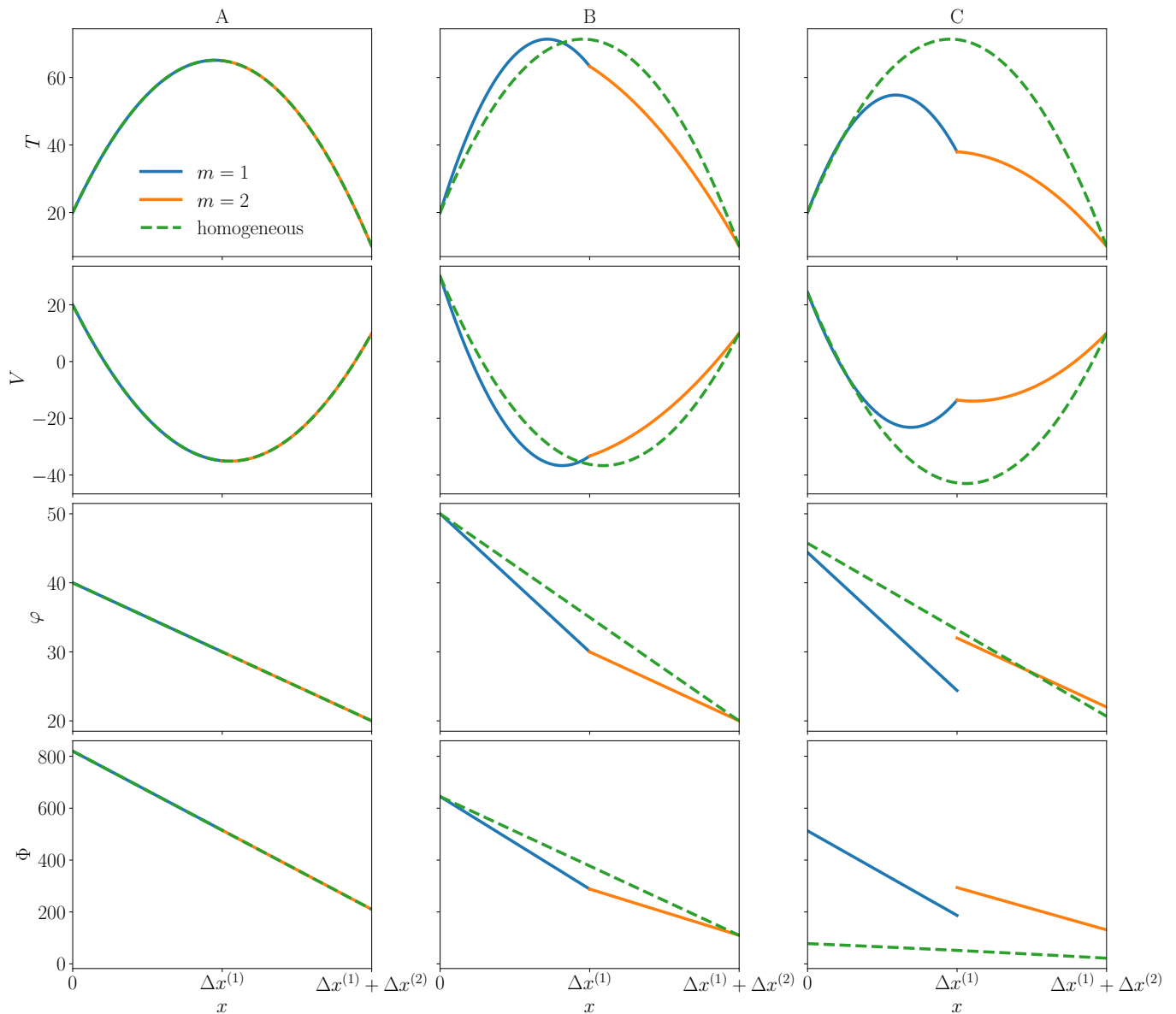


FIG. 4. Potential profiles derived in Appendix A 1 along the x direction (see Fig. 1) for TECs 1 (blue line) and 2 (orange line) of length $\Delta x^{(1)} = 1$ (respectively $\Delta x^{(2)} = 1$) and for a TEC of length $\Delta x^{(1)} + \Delta x^{(2)} = 2$ with thermoelectric coefficients $R^{(1)} + R^{(2)}, K^{(1)}K^{(2)}/(K^{(1)} + K^{(2)})$ (green dashed line). The plot legends located in the upper left panel applies to all panels. The first line of graphs corresponds to the temperature $T(x)$, the second line to the electric potential $V(x)$, the third line to the composite potential $\varphi(x)$ and the last line to the composite potential $\Phi(x)$. In each column, the set of thermoelectric coefficients for both TECs are fixed to particular values. Column A corresponds to TEC 1 and 2 with equal thermoelectric coefficients: $K^{(1)} = K^{(2)} = 1, R^{(1)} = R^{(2)} = 1, \alpha^{(1)} = \alpha^{(2)} = 1$. Column B corresponds to the weaker condition ensuring composite potential continuity (see section III C) with $K^{(1)} = 1, K^{(2)} = 2, R^{(1)} = 2, R^{(2)} = 1, \alpha^{(1)} = \alpha^{(2)} = 1$. Column C corresponds to TEC 1 and 2 with different thermoelectric coefficients $K^{(1)} = 1, K^{(2)} = 2, R^{(1)} = 2, R^{(2)} = 1, \alpha^{(1)} = 1, \alpha^{(2)} = 1.2$. We also fix the boundary conditions $T_l = 20, T_r = 10, V_r = 10, I_C = 5$.

than the manifestation of the Peltier effect at the junction between devices (1) and (2). In this case, the heat flow I_Q no longer directly follows the potential as before, and we see a discontinuity in the values of the potentials φ and Φ . This discontinuity corresponds to the Peltier heat current $I_{QP} = (\alpha_2 - \alpha_1) I_C$ exchanged at the junction. This contribution, positive in this case, results in

an increase in the values of the φ and Φ potentials at the junction, while the slopes remain identical to the previous case.

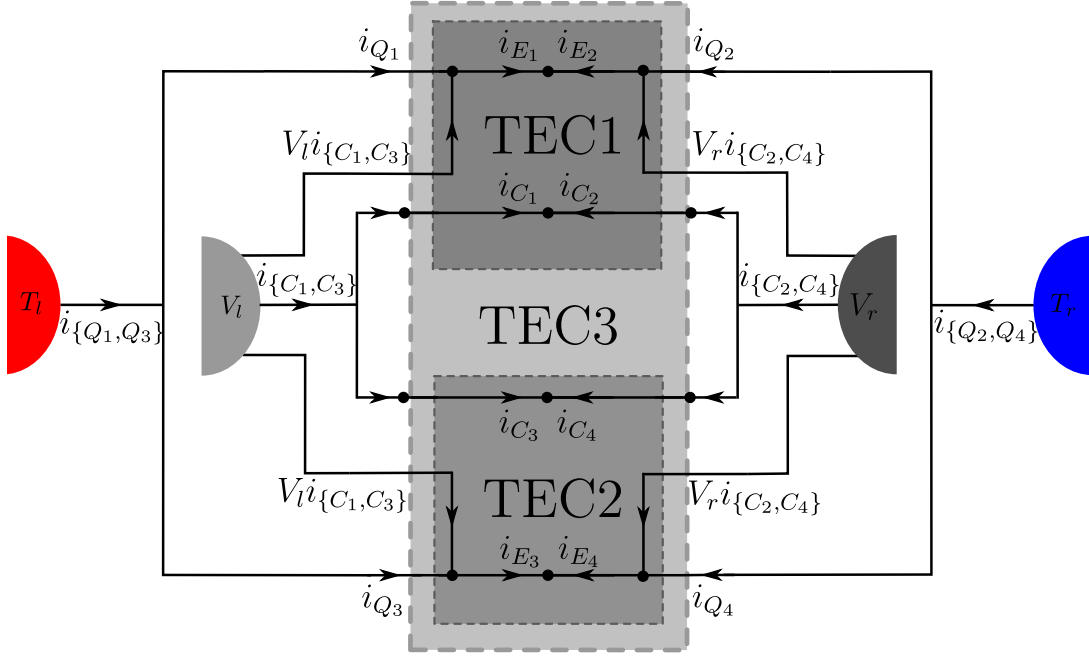


FIG. 5. TEC 3 is connected to two thermostats at temperatures T_l and T_r with $\Delta T^{(3)} = T_r - T_l < 0$ and to two metallic leads at electrical potentials V_l and V_r with $\Delta V^{(3)} = V_l - V_r > 0$. TEC 3 is the parallel association of TEC 1 and 2..

IV. PARALLEL ASSOCIATION

We now turn to the study of the parallel association of two TECs. Its equivalent current-force characteristics described by the equivalent conductance matrix is obtained in section IV A from the law of conductance matrix addition. We discuss the physics of the parallel association in section IV B. The conservation laws for the device resulting from the parallel association are studied in Appendix B.

The parallel association of two TECs is represented on Fig. 5. Following the pin ensemble definitions given in Ref. [13] for the parallel association, the pins of devices 1, 2 and 3 are

$$\mathcal{P}^{(1)} = \{E_1, C_1, E_2, C_2\}, \quad (44)$$

$$\mathcal{P}^{(2)} = \{E_3, C_3, E_4, C_4\}, \quad (45)$$

$$\mathcal{P}^{(3)} = \{\{E_1, E_3\}, \{C_1, C_3\}, \{E_2, E_4\}, \{C_2, C_4\}\}, \quad (46)$$

where E_i (resp. C_i) is the index of the pin number i associated to energy transport (to charge transport). We recall that the pins in $\mathcal{P}^{(3)}$ are called lumped pins. Each pin P in $\mathcal{P}^{(3)}$ gathers the pins in $\mathcal{P}^{(1)}$ and $\mathcal{P}^{(2)}$ that are set at the same local potential. This means that the local potentials at all pins of TEC 1 and 2 are functions of the potential on the lumped pin of device 3 as

$$\mathbf{a}^{(m)} = \boldsymbol{\pi}_{\parallel}^{(m,3)} \mathbf{a}^{(3)}, \quad (47)$$

for $m = 1, 2$, where the matrices $\boldsymbol{\pi}_{\parallel}^{(m,3)}$ read

$$\boldsymbol{\pi}_{\parallel}^{(1,3)} = \begin{bmatrix} 1 & 0 & 0 & 0 \\ 0 & 1 & 0 & 0 \\ 0 & 0 & 1 & 0 \\ 0 & 0 & 0 & 1 \end{bmatrix} \begin{matrix} E_1 \\ C_1 \\ E_2 \\ C_2 \end{matrix}, \quad (48)$$

$$\boldsymbol{\pi}_{\parallel}^{(2,3)} = \begin{bmatrix} 1 & 0 & 0 & 0 \\ 0 & 1 & 0 & 0 \\ 0 & 0 & 1 & 0 \\ 0 & 0 & 0 & 1 \end{bmatrix} \begin{matrix} E_3 \\ C_3 \\ E_4 \\ C_4 \end{matrix}. \quad (49)$$

These two matrices encode the topology of the parallel association of TEC 1 and 2. Given the symmetry of the association considered here they happen to be identical and equal to identity.

A. Equivalent conductance matrix

We now turn to the determination of the conductance matrix for device 3. We have shown in Ref. [9] that the conductance matrix at physical level for the internal currents of a single TEC (here for $m = 1, 2$) reads

$$\mathbf{g}_i^{(m)} = \begin{bmatrix} \mathbf{G}_i^{(m)} & -\mathbf{G}_i^{(m)} \\ -\mathbf{G}_i^{(m)} & \mathbf{G}_i^{(m)} \end{bmatrix} \quad (50)$$

where $\mathbf{G}_i^{(m)}$ is the conductance matrix recalled in Eq. (7). Now, using the law of conductance matrix addition derived in Ref. [13], the conductance matrix for device 3

reads

$$\mathbf{g}^{(3)} = \sum_{m=1}^2 \pi_{\parallel}^{(m,3)T} \mathbf{g}^{(m)} \pi_{\parallel}^{(m,3)} \quad (51)$$

and since for $m = 1, 2$ we have shown that $\pi_{\parallel}^{(m,3)} = \mathbb{1}_4$, $\mathbf{g}^{(3)}$ simplifies to

$$\mathbf{g}^{(3)} = \begin{bmatrix} \mathbf{G}^{(1)} + \mathbf{G}^{(2)} & -(\mathbf{G}^{(1)} + \mathbf{G}^{(2)}) \\ -(\mathbf{G}^{(1)} + \mathbf{G}^{(2)}) & \mathbf{G}^{(1)} + \mathbf{G}^{(2)} \end{bmatrix}. \quad (52)$$

The conductance matrix $\mathbf{G}^{(3)}$ for a set of linearly independent currents of devices 3, reads

$$\mathbf{G}^{(3)} = \mathbf{S}^{(3)+} \mathbf{g}^{(3)} \mathbf{S}^{(3)+T} \quad (53)$$

where $\mathbf{S}^{(3)}$ is the selection matrix that selects a set of independent currents among the redundant currents flowing through the pins in $\mathcal{P}^{(3)}$.

B. Discussion

Insofar as the parallel configuration preserves the Dirichlet conditions for each of the two devices, the electric linear behaviors are also preserved by simple application of the superposition theorem. It is therefore natural that device 3 should also behave in a perfectly linear fashion. No impedance matching issues arise here, there is therefore no potential continuity issues. But this observation does not exhaust the subject. Indeed, the parallel configuration requires that the two electric parts of the two devices be connected in parallel. In this case, a loop current flows between the two electric parts of the TECs, unless they each have the same voltage across their terminals. It's easy to see that the respective currents are given by:

$$i_{C_1} = -\frac{\delta\alpha\Delta T}{R^{(1)} + R^{(2)}} + \frac{R^{(2)}i_{\{C_1, C_2\}}}{R^{(1)} + R^{(2)}}, \quad (54)$$

$$i_{C_2} = \frac{R^{(1)}i_{\{C_1, C_2\}}}{(R^{(1)} + R^{(2)})} + \frac{\delta\alpha\Delta T}{R^{(1)} + R^{(2)}}, \quad (55)$$

where $i_{\{C_1, C_2\}} = i_{C_1} + i_{C_2}$. We can see that even when the current $i_{\{C_1, C_2\}}$ is zero, an electric current flows through both devices, generating residual internal dissipation. From these two equations it is clear that one of the devices will act as an electrical generator, feeding into the other. This is particularly obvious when we consider the $i_{\{C_1, C_2\}} = 0$ configuration. Once again, it is the presence of Seebeck coefficient difference between TECs 1 and 2 that leads to an unconventional situation. However, it's important to note that this time it's not a signature of the Peltier effect, unlike in the previous serial case.

V. CONCLUSION

Following previous works on the circuitation of TECs [16–18], we applied our general method for the serial and the parallel association of thermodynamic devices on the paradigmatic case of TECs. The law of resistance/conductance matrix addition takes in this case a simple form because of the symmetry of the associations and of the small number of pins. It thus paves the way for a systematic study of networks of thermoelectric since our toolbox is not limited to binary associations of TECs but can also be applied to more complex networks.

Our study unveiled in particular that the serial association of two TECs described by the CPM follows an effective CPM with electric current dependant thermoelectric coefficients. This emerges from non ideal boundary conditions, i.e., from the electric current dependency of the local potentials at their interface. The law of resistance addition (serial association) gives the proper modeling for the current-force characteristics of device 3: We obtain the same current-force characteristics whatever the method we use. However, the coupling between the currents is in principle predicted by the law of resistance addition. It is not however predicted by other approaches which prevents us from validating this part of our circuit theory on such thermodynamic models of TECs. In this regard, further investigations with stochastic modeling are required. A step in this direction is achieved in the fourth paper of this series dealing with chemical reaction networks.

In any case, it would be interesting to investigate the link between the nonequilibrium conductance matrix of a TEC with the fluctuations of its currents in the light of the results on Markov jump processes derived in Ref. [19]. There the authors show that the nonequilibrium matrix gives the best lower bound on the current covariance. Our circuit theory would then allow us to determine the best lower bound on the currents covariances of a composite TEC given the bounds on the current covariances of the sub-TECs.

Appendix A: Serial association

In this Appendix, we first provide the material and method leading to the potential profiles for each TECs within the serial association. We also apply the general method developed in the first paper of this series: First, to obtain the conservation laws for device 3; second to justify the equivalent resistance matrix of Eq.(22) from our law of resistance matrix addition.

1. Potential profiles in each TECs

We derive in this section the potential profiles in the TECs as a function of space. As in Ref. [9], we assume that each TEC is an effectively one-dimensional material

along the x direction (transverse direction is irrelevant). Moreover we assume that TEC 1 lays between $x = 0$ and $x = \Delta x^{(1)}$ and that TEC 2 lays between $x = \Delta x^{(1)}$ and $x = \Delta x^{(1)} + \Delta x^{(2)}$. We provide the derivation of the temperature and the electric potential from which the composite potential profiles φ and Φ follow. The temperature and the electric potential profiles in each TECs are obtained by solving respectively Domenicalli's equation

$$\frac{d^2 T^{(m)}}{dx^2} = -\frac{J_C^2}{\kappa_J^{(m)} \sigma_T^{(m)}}, \quad (\text{A1})$$

and

$$\frac{d^2 V^{(m)}}{dx^2} = \frac{\alpha J_C^2}{\kappa_J^{(m)} \sigma_T^{(m)}}, \quad (\text{A2})$$

where we have introduced the local charge flux J_C (in $C.s^{-1}$) positive when flowing toward positive x direction, the (local) thermal conductivity at null electric current $\kappa_J^{(m)}$ (in $W.m^{-1}.K^{-1}$) and the (local) isothermal electrical conductivity $\sigma_T^{(m)}$ (in $S.m^{-1}$). The thermal and the electric boundary conditions for TEC $m = 1, 2$ are respectively

$$T^{(1)}(0) = T_l, \quad T^{(1)}(\Delta x^{(1)}) = T, \quad (\text{A3})$$

$$T^{(2)}(\Delta x^{(1)}) = T, \quad T^{(2)}(\Delta x^{(1)} + \Delta x^{(2)}) = T_r, \quad (\text{A4})$$

and

$$V^{(1)}(0) = V_l, \quad V^{(1)}(\Delta x^{(1)}) = V, \quad (\text{A5})$$

$$V^{(2)}(\Delta x^{(1)}) = V, \quad V^{(2)}(\Delta x^{(1)} + \Delta x^{(2)}) = V_r. \quad (\text{A6})$$

T and V are respectively the temperature and the electric potential at the interface between the two materials. They are determined from the conservation of charge energy at the interface between TEC 1 and 2, see Section III A. Note that for TEC $m = 1, 2$, we use in the main text the integrated thermal and electrical conductivities [9]

$$R^{(m)} = \frac{\Delta x^{(m)}}{\sigma_T \mathcal{A}}, \quad K^{(m)} = \frac{\kappa_J \mathcal{A}}{\Delta x^{(m)}} \quad (\text{A7})$$

where \mathcal{A} is the surface across which the fluxes are counted and $\Delta x^{(m)}$ is the length of TEC m . The electric current across surface \mathcal{A} is defined as $I_C = \mathcal{A} J_C$. We thus reexpress Eqs. (A1–A2) as:

$$\frac{d^2 T^{(m)}}{dx^2} = A_T^{(m)} = -\frac{1}{\Delta x^{(m)2}} \frac{R^{(m)} I_C^2}{K^{(m)}}, \quad (\text{A8})$$

$$\frac{d^2 V^{(m)}}{dx^2} = A_V^{(m)} = \frac{1}{\Delta x^{(m)2}} \frac{\alpha^{(m)} R^{(m)} I_C^2}{K^{(m)}}, \quad (\text{A9})$$

	$m = 1$	$m = 2$
$B_T^{(m)}$	$\frac{\Delta T^{(1)} - A_T^{(1)} \Delta x^{(1)2}}{\Delta x^{(1)}}$	$\frac{\Delta T^{(2)} - A_T^{(2)} \Delta x^{(2)} (2\Delta x^{(1)} + \Delta x^{(2)})}{\Delta x^{(2)}}$
$C_T^{(m)}$	$T_l^{(1)}$	$T - A_T^{(2)} \Delta x^{(1)2} - B_T^{(2)} \Delta x^{(1)}$
$B_V^{(m)}$	$\frac{\Delta V^{(1)} - A_V^{(1)} \Delta x^{(1)2}}{\Delta x^{(1)}}$	$\frac{\Delta V^{(2)} - A_V^{(2)} \Delta x^{(2)} (2\Delta x^{(1)} + \Delta x^{(2)})}{\Delta x^{(2)}}$
$C_V^{(m)}$	$V_l^{(1)}$	$V - A_V^{(2)} \Delta x^{(1)2} - B_V^{(2)} \Delta x^{(1)}$

TABLE I. Integration constants for the integration of Eqs. (A8) and (A9).

where we have introduced the constants $A_T^{(m)}$ and $A_V^{(m)}$ (not to be confused with fundamental thermodynamic forces). The general solution of Eqs. (A8–A9) read

$$T^{(m)}(x) = A_T^{(m)} x^2 + B_T^{(m)} x + C_T^{(m)}, \quad (\text{A10})$$

$$V^{(m)}(x) = A_V^{(m)} x^2 + B_V^{(m)} x + C_V^{(m)}. \quad (\text{A11})$$

The integration constants (linear and constant terms) $B_a^{(m)}$ and $C_a^{(m)}$ for $m = 1, 2$ and $a = T, V$ are given in Table I. Those temperature and voltage profiles were used to draw Fig. 4.

2. Conservation laws

We start by defining the internal physical currents for each TEC $m = 1, 2, 3$

$$\mathbf{i}^{(m)} = \begin{pmatrix} i_{El}^{(m)} \\ i_{Cl}^{(m)} \\ i_{Er}^{(m)} \\ i_{Cr}^{(m)} \end{pmatrix}. \quad (\text{A12})$$

As illustrated in Fig. 2, the serial association of device 1 and 2 is such that $i_{El}^{(3)} = I_E$, $i_{Cl}^{(3)} = I_C$ and $i_{Er}^{(3)} = -I_E$, $i_{Cr}^{(3)} = -I_C$. This means that $\mathbf{i}^{(3)}$ reads:

$$\mathbf{i}^{(3)} = \begin{pmatrix} I_E \\ I_C \\ -I_E \\ -I_C \end{pmatrix}. \quad (\text{A13})$$

Conservation laws can be summarized in a matrix form as in Ref. [13]

$$\boldsymbol{\ell}^{(m)} \mathbf{i}^{(m)} = 0, \quad (\text{A14})$$

where

$$\boldsymbol{\ell}^{(m)} = [\mathbb{1}_2 \quad \mathbb{1}_2] \quad (\text{A15})$$

for $m = 1, 2$ and where $\mathbb{1}_2$ is the 2×2 identity matrix. For $m = 3$, the conservation laws are trivially the same by construction of $\mathbf{i}^{(3)}$ Eq. (A13). We now recover this

result by using the method developed in Ref. [13]. These conservation laws for $m = 1, 2$ can be gathered as

$$\begin{bmatrix} \mathbb{1}_2 & \mathbb{0}_2 \\ \mathbb{0}_2 & \mathbb{1}_2 \end{bmatrix} \mathbf{i}^{(3)} = - \begin{bmatrix} \mathbb{1}_2 & \mathbb{0}_2 \\ \mathbb{0}_2 & \mathbb{1}_2 \end{bmatrix} \begin{pmatrix} i_{Er}^{(1)} \\ i_{Cr}^{(1)} \\ i_{El}^{(2)} \\ i_{Cl}^{(2)} \end{pmatrix}. \quad (\text{A16})$$

Then, using the conservation of energy and charge at the interface Eqs. (9) and (10), we express Eq. (A16) in terms of $i_{Er}^{(1)}, i_{Cr}^{(1)}$ only as:

$$\mathbf{L}_e \mathbf{i}^{(3)} = \mathbf{L}_i \mathbf{i}_r^{(1)} \quad (\text{A17})$$

where we define

$$\mathbf{L}_e = \begin{bmatrix} \mathbb{1}_2 & \mathbb{0}_2 \\ \mathbb{0}_2 & \mathbb{1}_2 \end{bmatrix}, \quad \mathbf{L}_i = \begin{bmatrix} -\mathbb{1}_2 \\ \mathbb{1}_2 \end{bmatrix}, \quad (\text{A18})$$

and

$$\mathbf{i}_r^{(1)} = \begin{pmatrix} i_{Er}^{(1)} \\ i_{Cr}^{(1)} \end{pmatrix}. \quad (\text{A19})$$

As shown in Ref. [9], the conservation laws for device 3 are obtained by multiplying Eq. (A17) on the left by \mathbf{v} , the matrix in which the lines are the basis vector of coker(\mathbf{L}_i) such that $\mathbf{v} \mathbf{L}_i = \mathbf{0}$. This matrix \mathbf{v} reads

$$\mathbf{v} = (\mathbb{1}_2 \quad \mathbb{1}_2). \quad (\text{A20})$$

$\ell^{(3)}$ is thus readily found to be:

$$\ell^{(3)} = \mathbf{v} \mathbf{L}_e = (\mathbb{1}_2 \quad \mathbb{1}_2). \quad (\text{A21})$$

As expected from the symmetry of the serial association of TEC 1 and 2, the matrix of conservations for device 3 is the same as the one for device 1 and 2.

3. Conductance matrix dimension matching

For each devices $m = 1, 2, 3$, the vector of linearly dependent currents $\mathbf{i}^{(m)}$ follows from the vector of independent currents $\mathbf{I}^{(m)}$ as

$$\mathbf{i}^{(m)} = \mathbf{S}^{(m)} \mathbf{I}^{(m)} \quad (\text{A22})$$

where $\mathbf{S}^{(m)}$ is a selection matrix whose column vectors are chosen as basis vectors of $\ker(\ell^{(m)})$ such that $\ell^{(m)} \mathbf{S}^{(m)} = \mathbf{0}$. For all $m = 1, 2, 3$, we choose the following vector of linearly independent currents

$$\mathbf{I}^{(m)} = \begin{pmatrix} i_{El}^{(m)} \\ i_{Cl}^{(m)} \end{pmatrix} = \begin{pmatrix} I_E \\ I_C \end{pmatrix} \quad (\text{A23})$$

which is associated to the following choice of selection matrix and its associated pseudoinverse

$$\mathbf{S}^{(m)} = \begin{bmatrix} \mathbb{1}_2 \\ -\mathbb{1}_2 \end{bmatrix} \quad \text{and} \quad \mathbf{S}^{(m)+} = \frac{1}{2} (\mathbb{1}_2 \quad -\mathbb{1}_2). \quad (\text{A24})$$

In Ref. [13], we derived the current-force relation for device $m = 1, 2$

$$\mathbf{I}^{(m)} = \mathbf{G}^{(m)} \mathbf{A}^{(m)} \quad (\text{A25})$$

where

$$\mathbf{G}^{(m)} = \frac{T_l^{(m)} T_r^{(m)}}{R^{(m)} \bar{T}^{(m)}} \begin{bmatrix} K^{(m)} R^{(m)} \bar{T}^{(m)} + F^{(m)2} & F^{(m)} \\ F^{(m)} & 1 \end{bmatrix}. \quad (\text{A26})$$

and

$$\mathbf{A}^{(m)} = \begin{pmatrix} A_E^{(m)} \\ A_C^{(m)} \end{pmatrix} = \begin{pmatrix} \frac{1}{T_r^{(m)}} - \frac{1}{T_l^{(m)}} \\ \frac{V_l^{(m)}}{T_l^{(m)}} - \frac{V_r^{(m)}}{T_r^{(m)}} \end{pmatrix} \quad (\text{A27})$$

where $A_E^{(m)}$ (resp. $A_C^{(m)}$) is the affinity conjugated to the energy (resp. charge) current in the EPR. Following Ref. [13] to determine $\mathbf{G}^{(3)}$, we start solving Eq. (A17) for $\mathbf{i}_r^{(1)}$ which yields

$$\mathbf{i}_r^{(1)} = \frac{1}{2} [-\mathbb{1}_2 \quad \mathbb{1}_2] \mathbf{i}^{(3)} \quad (\text{A28})$$

where we used the left pseudo-inverse since the columns of \mathbf{L}_i are linearly independent. This last relation can thus be used to express $\mathbf{i}^{(m)}$ for $m = 1, 2$ in term of $\mathbf{i}^{(3)}$ as

$$\mathbf{i}^{(m)} = \boldsymbol{\pi}^{(m,3)} \mathbf{i}^{(3)}, \quad (\text{A29})$$

where

$$\boldsymbol{\pi}^{(1,3)} = \begin{bmatrix} \mathbb{1}_2 & \mathbf{0}_2 \\ -\frac{1}{2} \mathbb{1}_2 & \frac{1}{2} \mathbb{1}_2 \end{bmatrix}, \quad \boldsymbol{\pi}^{(2,3)} = \begin{bmatrix} \frac{1}{2} \mathbb{1}_2 & -\frac{1}{2} \mathbb{1}_2 \\ \mathbf{0}_2 & \mathbb{1}_2 \end{bmatrix}. \quad (\text{A30})$$

Now the law of resistance addition reads

$$\mathbf{R}^{(3)} = \sum_{m=1}^2 \boldsymbol{\Pi}^{(m,3)T} \mathbf{R}^{(m)} \boldsymbol{\Pi}^{(m,3)} \quad (\text{A31})$$

where

$$\boldsymbol{\Pi}^{(m,3)} \equiv \mathbf{S}^{(m)+} \boldsymbol{\pi}^{(m,3)} \mathbf{S}^{(3)} = \mathbb{1}_2. \quad (\text{A32})$$

We thus obtain

$$\mathbf{R}^{(3)} = \mathbf{R}^{(1)} + \mathbf{R}^{(2)}. \quad (\text{A33})$$

Appendix B: Parallel association: conservation laws

To determine $\ell^{(3)}$ in the case of a parallel association, we follow the method introduced in Ref. [13]. Eq. (A15) provides the conservation of internal currents for TEC 1 and 2, i.e., their conservation laws before parallel association. The external conservation laws, i.e. the conservation laws arising from the parallel association of TEC 1 and 2 to create TEC 3, are

$$\mathbf{i}^{(3)} = \left[\boldsymbol{\pi}_{\parallel}^{(1,3)T} \quad \boldsymbol{\pi}_{\parallel}^{(2,3)T} \right] \begin{pmatrix} \mathbf{i}^{(1)} \\ \mathbf{i}^{(2)} \end{pmatrix}, \quad (\text{B1})$$

where

$$\mathbf{i}^{(3)} = \begin{pmatrix} i_{\{E_1, E_3\}} \\ i_{\{C_1, C_3\}} \\ i_{\{E_2, E_4\}} \\ i_{\{C_2, C_4\}} \end{pmatrix}, \quad \begin{pmatrix} \mathbf{i}^{(1)} \\ \mathbf{i}^{(2)} \end{pmatrix} = \begin{pmatrix} i_{E_1} \\ i_{C_1} \\ i_{E_2} \\ i_{C_2} \\ i_{E_3} \\ i_{C_3} \\ i_{E_4} \\ i_{C_4} \end{pmatrix}. \quad (\text{B2})$$

We gather all these conservation laws as follow

$$\mathbf{L} \begin{pmatrix} \mathbf{i}^{(1)} \\ \mathbf{i}^{(2)} \\ \mathbf{i}^{(3)} \end{pmatrix} = \begin{pmatrix} 0 \\ 0 \\ 0 \\ 0 \end{pmatrix}, \quad (\text{B3})$$

where

$$\mathbf{L} = \left[\begin{array}{cccc|cccc} 1 & 0 & 1 & 0 & 0 & 0 & 0 & 0 \\ 0 & 1 & 0 & 1 & 0 & 0 & 0 & 0 \\ \hline 0 & 0 & 0 & 0 & 1 & 0 & 1 & 0 \\ 0 & 0 & 0 & 0 & 0 & 1 & 0 & 1 \\ \hline 1 & 0 & 0 & 0 & 1 & 0 & 0 & 0 \\ 0 & 1 & 0 & 0 & 0 & 1 & 0 & 0 \\ 0 & 0 & 1 & 0 & 0 & 0 & 1 & 0 \\ 0 & 0 & 0 & 1 & 0 & 0 & 0 & 1 \end{array} \right]. \quad (\text{B4})$$

A left null basis of \mathbf{L} reads

$$\mathbf{u} = \begin{bmatrix} -1 & 0 & -1 & 0 & 1 & 0 & 1 & 0 \\ 0 & -1 & 0 & -1 & 0 & 1 & 0 & 1 \end{bmatrix}. \quad (\text{B5})$$

Then, as proven in Ref. [13], left multiplying Eq. (B3) by \mathbf{u} shows that the last $|\mathcal{P}^{(3)}| = 4$ columns of \mathbf{u} gives the matrix of conservation laws for device 3 as

$$\boldsymbol{\ell}^{(3)} = \begin{pmatrix} 1 & 0 & 1 & 0 \\ 0 & 1 & 0 & 1 \end{pmatrix}. \quad (\text{B6})$$

Thus, TEC 3 made out of the parallel association of TEC 1 and 2 admits the same conservation laws, which was expected by symmetry.

-
- [1] T Teorell, “On the Thermodynamics of Irreversible Processes,” *Journal of Theoretical Biology* **3**, 1–3 (1953).
- [2] L Michaelis, “Thermodynamics of irreversible processes,” *The Journal of General Physiology* **13**, 629–649 (1930).
- [3] Lars Onsager, “Reciprocal relations in irreversible processes. i.” *Phys. Rev.* **37**, 405–426 (1931).
- [4] Aharon Katchalsky and Peter F Curran, *Nonequilibrium thermodynamics in biophysics* (Harvard University Press, 1965).
- [5] George F. Oster, Alan S. Perelson, and Aharon Katchalsky, “Network thermodynamics: dynamic modelling of biophysical systems,” *Quarterly Reviews of Biophysics* **6**, 1–134 (1973).
- [6] O Kedem and S Roy Caplan, “Degree of coupling and its relation to efficiency of energy conversion,” *Transactions of the Faraday Society* **61**, 1897–1911 (1965).
- [7] H.A. Kramers, “Brownian motion in a field of force and the diffusion model of chemical reactions,” *Physica* **7**, 284–304 (1940).
- [8] Y. Apertet, H. Ouerdane, C. Goupil, and Ph. Lecoeur, “From local force-flux relationships to internal dissipations and their impact on heat engine performance: The illustrative case of a thermoelectric generator,” *Physical Review E* **88**, 022137 (2013).
- [9] Paul Raux, Christophe Goupil, and Gatien Verley, “Thermodynamic circuits 2: Nonequilibrium conductance matrix for a thermoelectric converter,” (2024), 10.48550/ARXIV.2405.11886, arXiv:2405.11886 [cond-mat.stat-mech].
- [10] G. Jeffrey Snyder and Tristan S. Ursell, “Thermoelectric efficiency and compatibility,” *Phys. Rev. Lett.* **91**, 148301 (2003).
- [11] Christophe Goupil, Wolfgang Seifert, Knud Zabrocki, Eckhart Müller, and G. Jeffrey Snyder, “Thermodynamics of thermoelectric phenomena and applications,” *Entropy* **13**, 1481–1517 (2011).
- [12] Christophe Goupil, “Thermodynamics of the thermoelectric potential,” *Journal of Applied Physics* **106**, 104907 (2009), <https://pubs.aip.org/aip/jap/article-pdf/doi/10.1063/1.3257250/15051079/104907.1.online.pdf>.
- [13] Paul Raux, Christophe Goupil, and Gatien Verley, “Thermodynamic circuits: Association of devices in stationary nonequilibrium,” *Physical Review E* **110**, 014134 (2024).
- [14] Christophe Goupil, Henni Ouerdane, Eric Herbert, Clémence Goupil, and Yves D’Angelo, “Thermodynamics of metabolic energy conversion under muscle load,” *New Journal of Physics* **21**, 023021 (2019).
- [15] Note that $R_{22}^{(3)'} - R_{22}^{(3)}$ reads
- $$\begin{aligned} R_{22}^{(3)'} - R_{22}^{(3)} &= 2 \frac{KR\bar{T}^{(3)} + F^{(3)2}}{KT_l T_r} \\ &\quad - \frac{KR\bar{T}^{(1)} + F^{(1)2}}{KT_l T} - \frac{KR\bar{T}^{(2)} + F^{(2)2}}{KTT_r} \\ &= \frac{1}{K} \left(\frac{F^{(1)2} + F^{(2)2}}{2T_l T_r} - \frac{1}{T} \left\{ \frac{F^{(1)2}}{T_l} + \frac{F^{(2)2}}{T_r} \right\} \right) \\ &\quad + \frac{F^{(1)}F^{(2)}}{T_l T_r} + \frac{R}{2} (A_E^{(2)} - A_E^{(1)}) \end{aligned} \quad (\text{B7})$$
- [16] Y. Apertet, H. Ouerdane, C. Goupil, and Ph. Lecoeur, “Thermoelectric internal current loops inside inhomoge-

- neous systems,” [Physical Review B](#) **85**, 033201 (2012).
- [17] Y. Apertet, H. Ouerdane, C. Goupil, and Ph. Lecoeur, “Efficiency at maximum power of thermally coupled heat engines,” [Physical Review E](#) **85**, 041144 (2012).
- [18] Y. Apertet, H. Ouerdane, O. Glavatskaya, C. Goupil, and P. Lecoeur, “Optimal working conditions for thermoelectric generators with realistic thermal coupling,” [EPL \(Europhysics Letters\)](#) **97**, 28001 (2012).
- [19] Hadrien Vroylandt, David Lacoste, and Gatien Verley, “Degree of coupling and efficiency of energy converters far-from-equilibrium,” [Journal of Statistical Mechanics: Theory and Experiment](#) **2018**, 023205 (2018).